

RSC Advances

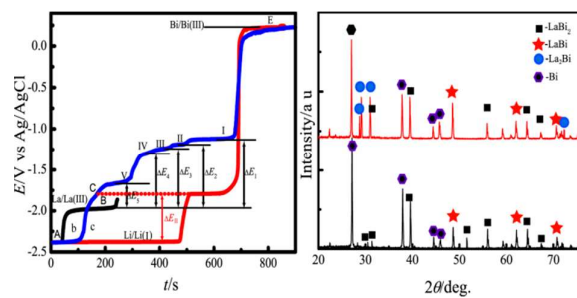


This is an *Accepted Manuscript*, which has been through the Royal Society of Chemistry peer review process and has been accepted for publication.

Accepted Manuscripts are published online shortly after acceptance, before technical editing, formatting and proof reading. Using this free service, authors can make their results available to the community, in citable form, before we publish the edited article. This *Accepted Manuscript* will be replaced by the edited, formatted and paginated article as soon as this is available.

You can find more information about *Accepted Manuscripts* in the [Information for Authors](#).

Please note that technical editing may introduce minor changes to the text and/or graphics, which may alter content. The journal's standard [Terms & Conditions](#) and the [Ethical guidelines](#) still apply. In no event shall the Royal Society of Chemistry be held responsible for any errors or omissions in this *Accepted Manuscript* or any consequences arising from the use of any information it contains.



Electrochemical behavior of La(III) was studied on liquid Bi electrode. Thermodynamic properties of five La-Bi intermetallic compounds and Li_3Bi were calculated from emf measurements.



Journal Name

ARTICLE

Electrochemical behaviour of La(III) on liquid Bi electrode in LiCl-KCl melts. Determination of thermodynamic properties of La-Bi and Li-Bi intermetallic compounds

Received 00th January 20xx,
Accepted 00th January 20xx

DOI: 10.1039/x0xx00000x

Mei Li, Qunqun Gu, Wei Han, Xingmei Zhang, Yang Sun, Milin Zhang, Yongde Yan

www.rsc.org/

Electrochemical behavior of La(III) was studied on liquid Bi electrodes (i.e Bi pool and Bi coated W electrodes) in LiCl-KCl melts using cyclic voltammetry, square wave voltammetry, chronopotentiometry and open circuit chronopotentiometry. In both the electrodes, the electrochemical reduction of La(III) was observed at more positive potential values than that on an inert W electrode, due to the lowering of the activity of La in liquid Bi phase. Cyclic voltammetry, using a Bi pool electrode, suggests that the reduction of La(III) to La in liquid Bi was a quasi-reversible and diffusion controlled process. The diffusion coefficient of La in liquid Bi metal was measured by chronopotentiometry at 773 K and was evaluated by Sutherland-Einstein equation, respectively. Both the values of diffusion coefficient were of the same order of magnitude. From cyclic voltammogram and square wave voltammogram obtained on Bi coated W electrode, five couples of cathodic peaks were observed at more positive potential than that for La metal on an inert electrode due to the formation of five La-Bi intermetallic compounds. Thermodynamic properties such as activities and relative partial molar Gibbs energies of M (M=La, Li) in the M-Bi alloys as well as Gibbs energies of formation for M-Bi (M=La, Li) intermetallic compounds, LaBi₂, LaBi, La₃Bi₄, La₅Bi₃, La₂Bi and Li₃Bi were calculated from the open circuit potential measurement. La-Bi and La-Li-Bi alloys were produced on liquid Bi pool electrodes by galvanostatic and potentiostatic electrolysis, and characterized by X-ray diffraction (XRD) and scanning electronic microscopy (SEM). The results indicated that La-Bi alloys were comprised of LaBi₂, LaBi and La₂Bi phases, and LaBi₂, LaBi and Li₃Bi phases existed in La-Li-Bi alloys.

Introduction

Pyrometallurgical process is one of the most promising options for the reprocessing of advanced nuclear fuels and transmutation blankets which have high burn up potential and expected to have a high Pu and minor actinide contents.¹⁻⁴ Electrorefining⁵⁻⁸ and liquid-liquid metal reductive extraction^{8,9} are the most developed pyrochemical techniques intended for separation of actinides from fission products in molten salt media. Since the use of liquid metal electrodes has many advantages, such as complete physical separation between the electrolyte and the produced metal, constant surface area of the electrode, and easier coalescence of microdrops and metallic fog, the studies on liquid metals as working electrode are being extensively used to nuclear applications for pyrochemical reprocessing of irradiated nuclear fuels.¹⁰⁻²⁴ Gibilaro et al.¹⁰ investigated the electrochemical properties of various liquid metallic electrodes (Bi, Sb, Sn, Pb, Ga) in LiF-NaF and LiF-CaF₂ melts. They found the reactivity and nobility scale of liquid metallic

electrodes are in the order: Sb>Bi>Pb>Sn>Ga>Mo and Ga<Sn<Pb<Sb<Bi<Mo, respectively, by linear sweep voltammetry techniques. Murakami and Koyama¹¹ evaluated the diffusion coefficients of rare-earths (La, Pr, Nd, Gd, Y and Sc) in liquid Cd metal from the results of chronopotentiometry. The electrochemical behavior of Ce(III)¹², Pr(III)¹³, Nd(III)¹⁴, Tb(III)¹⁵, U(III)^{16,17}, Pu(III)^{17,18} and Np(III)¹⁹ were investigated on a liquid Cd electrode in molten LiCl-KCl eutectic. Castrillejo et al.^{13,15} evaluated the thermodynamic properties of the formation for the Tb-Cd and Pr-Cd intermetallic compounds by emf measurements. Vandarkuzhali et al.¹⁴ studied the apparent standard electrode potentials of Nd(III)/Nd for different temperatures in the range 698-773K. The formation of intermetallic, Cd₁₁Nd, was studied from open circuit potential measurement on a Cd film electrode. Kato et al.²⁰ investigated the separation behavior of actinides from rare-earths in molten salt electrorefining using saturated liquid cadmium cathode. The separation factors were calculated, and the values of separation factors were 0.011, 0.044, and 0.064 for La, Ce, Pr, and Nd, respectively. Castrillejo et al.^{13, 21} explored the electrode reactions of LiCl-KCl-PrCl₃ and LiCl-KCl-CeCl₃ solutions at the surface of liquid Bi electrode by electrochemical techniques. Emf measurements on various intermetallic compounds in two-phase coexisting states were carried out. The thermodynamic properties of formation for intermetallic compounds of Pr-Bi and Ce-Bi were

Key Laboratory of Superlight Materials and Surface Technology, Ministry of Education, College of Material Science and Chemical Engineering, Harbin Engineering University, Harbin 150001, China. Email: weihan@hrbeu.edu.cn; Tel.: +86 451 8256 9890; fax: +86 451 8253 3026

DOI: 10.1039/x0xx00000x

calculated, respectively. Shirai et al.^{19,22} studied the electrochemical behaviors of Pu(III)/Pu and Np(III)/Np couples at the interface between the LiCl-KCl and liquid Bi metal. The electrochemical behavior of the Th(IV)/Th system was examined in molten LiF-CaF₂ medium²³ and LiCl-KCl eutectic²⁴ on a liquid Bi film electrode, and the Bi-Th alloys were obtained. To the best of our knowledge, fundamental studies on the mechanism of electrode reaction and thermochemical data are not much reported on liquid Bi electrode.

Lanthanum, as the first element in the lanthanide series, having the closest ionic radius to U (III) among lanthanides, is a typical fission product and difficult to be separated from actinides. Therefore, it has been extensively studied on different cathodes, such as W²⁵⁻²⁸, Mo^{29,30}, Al²⁸, Cd^{11,20,31} and Bi film³² electrodes in molten salts. Serp et al.³² studied the electroseparation of plutonium from lanthanum using a Bi film electrode in LiCl-KCl eutectic at 733 K. The reduction potentials of Pu(III) and La(III) ions were measured on a Bi thin film electrode using cyclic voltammetry. They found that the difference between the peak potentials for the formation of PuBi₂ and LaBi₂ was approximately 100 mV and Pu could be efficiently deposited and separated from lanthanum.

However, there is sparse information about the electrochemical behaviors of La on liquid electrodes. In order to better understand the electrochemical reactions of La(III) on liquid electrodes, further acquisition of basic electrochemical and thermodynamic data on La in LiCl-KCl system is needed. Therefore, in the present paper, we explored the electrochemical behavior of La(III) on a liquid Bi pool electrode and a Bi coated W electrode, the diffusion coefficients of La in liquid Bi metal, as well as the thermodynamic properties of La-Bi and Li-Bi intermetallic compounds were determined by means of electrochemical techniques.

Experimental

Preparation and purification of the melts

The eutectic mixture of LiCl-KCl (45.8:54.2 mass, analytical grade) was first dried under vacuum for more than 72 h at 473 K to remove excess water and then melted in an alumina crucible placed in a quartz cell located in an electric furnace. Other impurities in the melts were removed by pre-electrolysis at -2.0 V (vs Ag/AgCl) for 3 h. La (III) ions were introduced into the bath in the form of dehydrated LaCl₃ powder (analytical grade). Since Ln ions are very sensitive to O²⁻ ions, in order to avoid the oxidation of La (III), HCl was bubbled to the melts to purify the melts and then argon was bubbled to remove the excess HCl.³³ The temperature of the melts was measured with a nickel chromium-nickel aluminum thermocouple sheathed by an alumina tube. All experiments were performed under an argon atmosphere.

Electrochemical apparatus and electrodes

All electrochemical measurements were performed using an Autolab PGSTAT 302N (Metrohm, Ltd.) with Nova 1.8 software where techniques of cyclic voltammetry (CV), square wave voltammetry (SWV), chronopotentiometry (CP) and open circuit chronopotentiometry (OCP) were employed. A silver wire ($d=1$ mm) dipped into a solution of AgCl (1 wt %) in the LiCl-KCl melts contained in a Pyrex tube was used as the reference electrode. All

potentials were referred to this Ag/AgCl couple. Different working electrodes have been used: (i) Bi pool electrode, (ii) liquid Bi electrode containing La, (iii) tungsten wire ($d = 1$ mm, 99.99 %) in order to compare the results with the liquid electrode. A spectral pure graphite rod ($d = 6$ mm) was used as the counter electrode.

The liquid Bi pool electrode (shown in Fig. 1) was prepared by placing some granules of Bi (99.999%) in a J shaped Pyrex tube, which was immersed in the LiCl-KCl melts. Contact was established by using a W wire ($d = 1$ mm, 99.99 %) immersed in the liquid Bi phase through the Pyrex tube.

The liquid Bi electrode containing La was prepared by potentiostatic electrolysis. The concentration of La in liquid Bi phase (C_{La}) was kept lower than its solubility. Assuming that the current efficiency of reaction on a liquid Bi pool electrode would be 100 %, C_{La} could be calculated. The C_{La} values measured by inductively coupled plasma-atomic emission spectrometer (ICP-AES) after experiments, agreed well with the values calculated under the above assumption. Thus the assumption was considered to be appropriate.

Molten salts electrolysis and characterization of deposits

The deposits were prepared by potentiostatic and galvanostatic electrolysis, respectively. After electrolysis, the alloy samples were washed in hexane (99.8 %) in an ultrasonic bath to remove salts and stored in a glove box for analysis. These deposits were analyzed by X-ray diffraction (XRD, X' Pert Pro; Philips Co., Ltd.) using Cu K α radiation at 40 kV and 40 mA. The specimen was mounted in thermosetting resins using a metallographic mounting press and then mechanically polished. And then, the microstructure was measured using scanning electronic microscopy (SEM, JSM-6480A; JEOL Co., Ltd.).

Results and discussion

The electrochemical behavior of La(III) on a liquid Bi pool electrode in LiCl-KCl melts

Cyclic Voltammetry. If the amount of La deposited exceeds its solubility in liquid Bi, solid phases would separate which results in that electrode losing its homogeneity and the voltammetric response would become less accurate. Therefore, it is very important to control the electrode surface and the La(III) concentration in the melts.

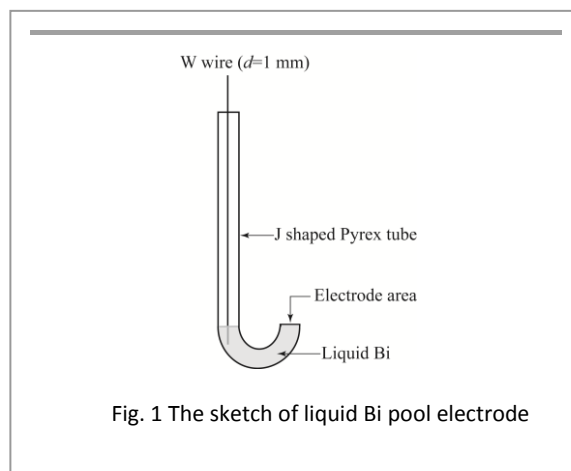


Fig. 1 The sketch of liquid Bi pool electrode

Fig. 2 presents the cyclic voltammograms obtained in LiCl-KCl melts on a W electrode and a liquid Bi pool electrode before and after the addition of ($5.2 \times 10^{-5} \text{ mol cm}^{-3}$) LaCl_3 , respectively. In curve a (black line), one couple of cathodic/anodic signals is observed at approximately -2.40/-2.22 V (vs Ag/AgCl). In such a negative potential, only metal cation/metal can obtain/lose electron in LiCl-KCl melts. Thus, the cathodic /anodic signals, A/A', correspond to the reduction of Li (I) and the re-oxidation of Li metal, respectively.

Curve b (red line) shows the cyclic voltammograms of LaCl_3 ($5.2 \times 10^{-5} \text{ mol cm}^{-3}$) in LiCl-KCl melts on a W electrode at 773 K. The signals B/B', at -2.04/-1.98 V, correspond to the deposition of La(III) and dissolution of La, respectively, which are consistent with those obtained by Tang and Pesic.³⁰



The typical cyclic voltammograms of LiCl-KCl melts on a liquid Bi electrode is presented in curve c (green line). Compared with curve a (black line), two new pairs of reduction/oxidation peaks are observed. Except the E' corresponding to the anodic dissolution of liquid Bi electrode, the signals C/C', at -1.40/-1.31 V, should be attributed to the deposition of Bi-Li alloy and subsequent dissolution of deposits.²¹



After the addition of LaCl_3 in LiCl-KCl melts, the typical cyclic voltammograms obtained on a liquid Bi electrode is presented in curve d (blue line). The voltammograms consist of a single cathodic wave D, at -1.13 V, associated with an anodic wave D', at -0.98 V, at potential values less cathodic than those obtained on an inert W electrode, due to a lowering of the activity of the dissolved La in liquid Bi phase as described in Eq. (4).



$$E = E_{\text{La(III)/La}}^0 + \frac{RT}{3F} \ln \frac{a_{\text{La(III) in melts}}}{a_{\text{La in liquid Bi}}} \quad (4)$$

The shape of the voltammograms is that expected for a soluble-soluble exchange. The results also suggest that the solubility of La in

the liquid Bi metal has not been achieved in the potential region below -1.2 V. A similar conclusion has been reported by Castrilleje et al.²³ in the case of Ce(III) electroreduction in liquid Bi metal.

Fig. 3 shows a series of the voltammograms obtained in LiCl-KCl- LaCl_3 melts on a Bi pool electrode, without formation of intermetallic compounds, at different scan rates. Furthermore, a further analysis of the recorded voltammograms is based on the measurement of the variation of peak currents and peak potentials with scan rates. Fig. 4a presents the linear relationship between the reduction peak current and the square root of the scan rate. The straight line through the origin proved that the reduction process is limited by mass transport both in the salt and the metallic phase. The reversibility of the system is examined by plotting the influence of the scan rate on the peak potential as presented in the Fig. 4b. At scan rate lower than 0.03 V s^{-1} , the peak potential, E_p , is constant and independent of the scan potential rate. Whereas for higher scan rates, the values of the anodic and cathodic peak potentials shift slightly towards positive and negative ones. These results indicate that the reduction of La (III) on a liquid Bi electrode is quasi-reversible above 0.03 V s^{-1} scan rate.

Chronopotentiometry. Chronopotentiometry was carried out at various anodic currents using the prepared liquid Bi electrode to evaluate the diffusion coefficient of La in liquid Bi metal. Since the formation of intermetallic compounds (i.e. La-Bi and Li-Bi intermetallic compounds) should lead to the morphology change of the liquid Bi metal surface, potentiostatic electrolysis was performed at -1.20 V for 2.5 h to prepare a liquid Bi electrode containing La. Fig. 5 displays the chronopotentiograms obtained on the prepared liquid Bi electrode at 773 K. In each chronopotentiogram, there is one potential plateau at around -0.97 V corresponding to the oxidation of La dissolved in liquid Bi metal (Eq. (3)). After the concentration of La near the surface of the liquid Bi electrode reached zero at $t = \tau$ (transition time), the potential changed steeply toward the Bi metal dissolution potential (the standard electrode potential of Bi(III)/Bi is about 0.22 V in LiCl-KCl melts at 773 K). The chronopotentiometry was terminated before the potential would reach the Bi metal dissolution potential to avoid the loss of liquid Bi metal. Transition time (τ) for each chronopotentiogram was evaluated and these values are listed in Table 1 together with the electrolysis conditions. In order to confirm that τ was given by the diffusion limit of solute La in liquid metal Bi not by the diffusion limit of La(III) in LiCl-KCl melts, in this study, chronopotentiometry was performed at a constant concentration of La(III) in LiCl-KCl melts and at several C_{La} . The

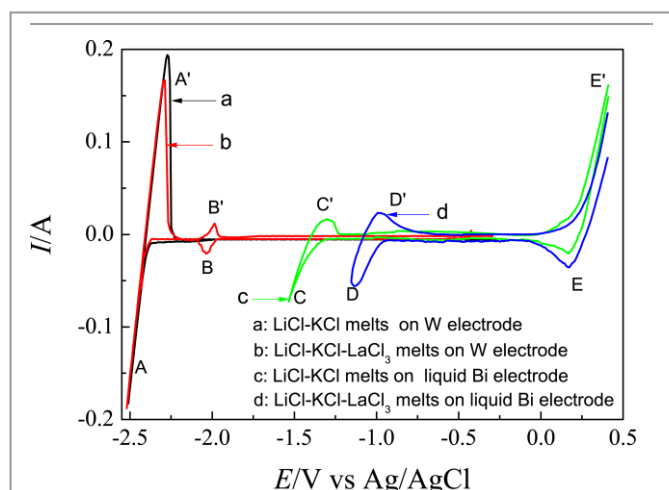


Fig. 2 Cyclic voltammograms obtained in LiCl-KCl melts on a W (curve a) and a Bi pool electrodes (curve c) before (curve b) and after (curve d) the addition of LaCl_3 ($5.2 \times 10^{-5} \text{ mol cm}^{-3}$) at 773 K. Scan rate: 0.1 V s^{-1} ; Electrode area: $S_W = 0.314 \text{ cm}^2$; $S_{\text{Bi}} = 0.2 \text{ cm}^2$.

Table 1 Experimental conditions of chronopotentiometry and evaluated transition time (s) for La at 773 K.

Applied current/A	$C_{\text{La}} \times 10^{-4} / \text{mol cm}^{-3}$	τ / s
0.03	7.584	13.114
0.031	7.545	10.856
0.032	7.511	10.03
0.034	7.479	9.55
0.036	7.447	6.75

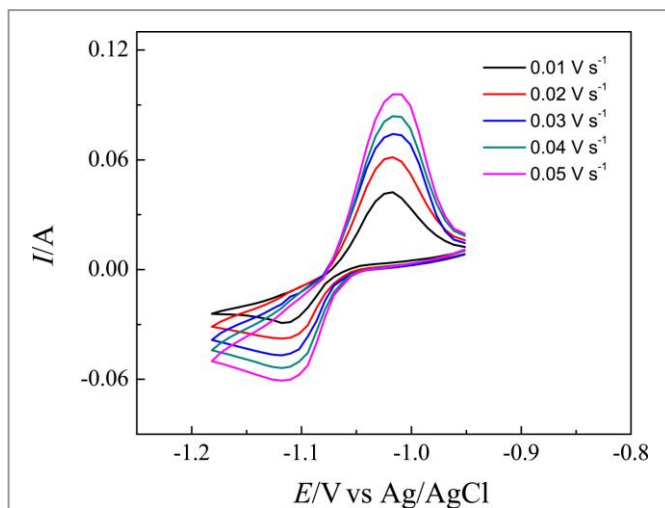


Fig. 3 Cyclic voltammograms obtained in LiCl-KCl-LaCl₃ (5.2×10^{-5} mol cm⁻³) melts on a liquid Bi pool electrode ($S=0.2$ cm²) at different scan rates at 773 K.

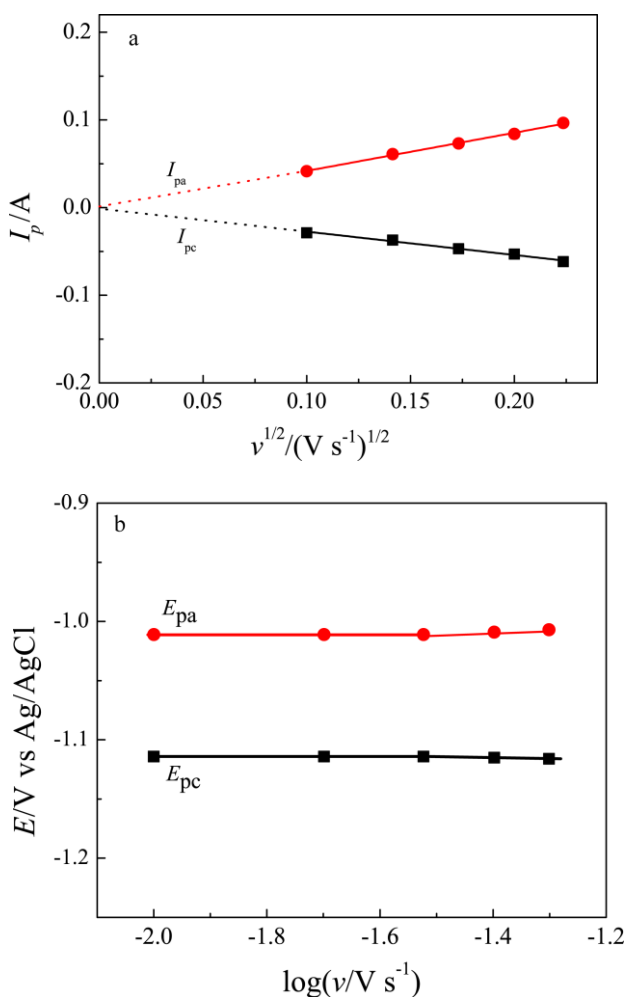


Fig. 4(a) Variation of the cathodic and anodic peak currents with the square root of the scan rates; (b) Variation of the cathodic and anodic peak potentials with the logarithm of the scan rates on a liquid Bi pool electrode at 773 K.

linear dependence of the $\tau^{1/2}$ on the concentration of La in liquid Bi metal (C_{La}) divided by the applied current (I) was confirmed that was given by the diffusion limit of solute La in liquid Bi (Fig. 5b). Then the diffusion coefficient, D_{La} can be calculated by applying Eq. (5):^{11,34}

$$I\tau^{1/2} = \frac{nFSC_{La}D_{La}^{1/2}\pi^{1/2}}{2} \quad (5)$$

Where I denotes the applied current (A), τ represents the transition time (s), D_{La} designates the diffusion coefficient of La in liquid Bi metal (cm² s⁻¹), S is the apparent electrode area and C_{La} corresponds to the initial concentrations of solute La in liquid metal (mol cm⁻³). Therefore, the value of D_{La} was calculated to be 1.81×10^{-5} cm² s⁻¹ at 773 K.

We also estimated the diffusion coefficient of La in liquid Bi metal, according to Sutherland-Einstein equation:³⁵

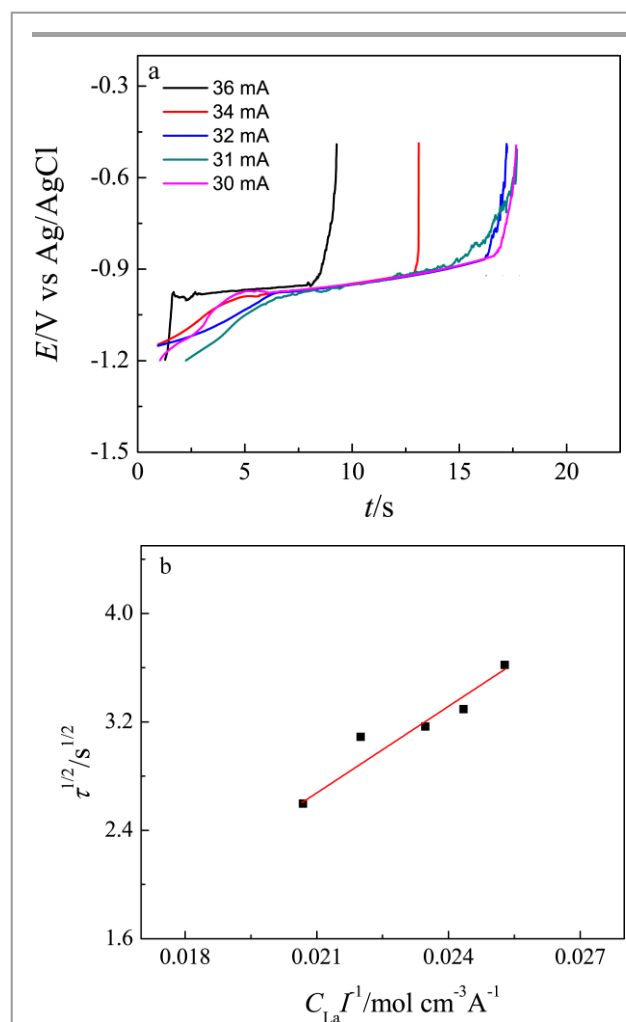


Fig. 5(a) Chronopotentiograms using a liquid Bi electrode containing La in LiCl-KCl-LaCl₃ (5.2×10^{-5} mol cm⁻³) melts at 773 K. The applied current: 30 mA, 31 mA, 32 mA, 34 mA, and 36 mA. $S_{Bi}=0.2$ cm²; (b) Plots for square root of transition time ($\tau^{1/2}$) against the concentration of La in liquid Bi metal (C_{La}) divided by the applied current (I).

$$D = kT / 4\pi r\eta \quad (6)$$

Where k denotes the Boltzmann constant ($1.38 \times 10^{-23} \text{ J K}^{-1}$), r represents solute radius ($r_{\text{La}} = 1.877 \times 10^{-8} \text{ cm}$), η designates the viscosity of the alloy (Pa s). Because the concentration of La in liquid Bi (C_{La}) is very low (lower than its solubility), the viscosity of Bi was substituted for that of La-Bi alloy. The viscosity of Bi was calculated by Eq. (7):³⁶

$$\eta_{\text{Bi}} = 4.458 \times 10^{-4} e^{775.8/T} \quad (7)$$

Combining Eq. (6) and (7), the value of diffusion coefficient of La (D_{La}) in liquid Bi was calculated to be $3.72 \times 10^{-5} \text{ cm}^2 \text{ s}^{-1}$ which is in the same order of magnitude to that obtained by chronopotentiometry.

Electrochemical behavior of La (III) on a Bi coated W electrode in LiCl-KCl-LaCl₃ melts

According to the La-Bi binary phase diagram,³⁷ there are five La-Bi intermetallic compounds, LaBi₂, LaBi, La₄Bi₃, La₅Bi₃ and La₂Bi in the La-Bi system. In order to obtain thermodynamic information concerning formation process of La-Bi intermetallic compounds, the electrochemical behavior of La(III) on a W electrode coated with a thin film of Bi has been studied by cyclic voltammetry, square wave voltammetry, and open circuit chronopotentiometry.

Cyclic voltammetry. Comparison of the cyclic voltammograms obtained in LiCl-KCl-BiCl₃ before and after the addition of LaCl₃ is displayed in Fig. 6a. In the LiCl-KCl-BiCl₃ melts, except for the peaks A/A', corresponding to the reduction/re-oxidation of Li, two pairs of peaks, C/C' and E/E', are observed. Cathodic peak E at around 0.18 V and its corresponding anodic peak E' at about 0.22 V should be ascribed to the deposition/dissolution of Bi metal, respectively. The results are consistent with those obtained in Fig. 1. Signals C/C', between signals of A/A' and E/E', correspond to the formation of a Li-Bi intermetallic by under-potential deposition of Li on the pre-deposition Bi which already covered the W electrode, i.e. Bi coated W electrode.

After the addition of LaCl₃ ($8.67 \times 10^{-5} \text{ mol cm}^{-3}$) in LiCl-KCl-BiCl₃ melts (red line in Fig. 6a), the voltammogram is more complex than that obtained on a liquid Bi pool electrode. In addition to the peaks A/A', C/C' and E/E', peaks B/B' can be ascribed to the reduction of La(III) to metal and its subsequent re-oxidation, respectively, according to the above results of LiCl-KCl-LaCl₃ melts on a W electrode (red line in Fig. 2). Between the peaks B/B' and E/E', a series of redox couples are ascribed to the formation/dissolution of different intermetallic compounds. In order to associate the dissolution anodic peaks with their corresponding cathodic formation, the voltammograms were registered at different inversion cathodic potentials, and the results are shown in Fig. 6b. Five new anodic peaks, I', II', III', IV' and V' observed correspond to the formation of five La-Bi intermetallic compounds, respectively. Since reduction peak potentials of I, II, and III are very close, the three cathodic peaks overlap each other. We can't distinguish the three cathodic peaks, respectively.

Square wave voltammetry. In order to distinguish the three cathodic peaks, I, II and III, a more sensitive technique, namely,

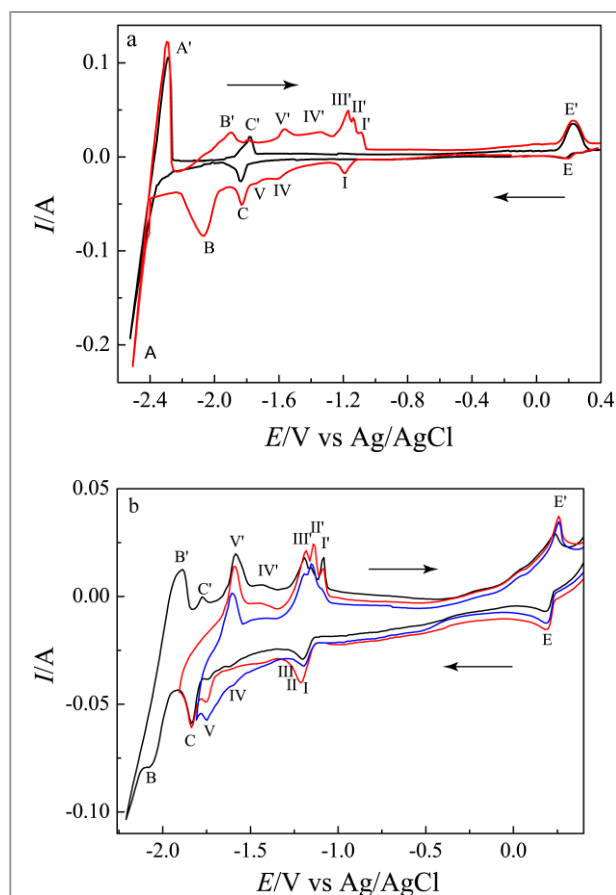


Fig. 6 (a) Cyclic voltammograms obtained on a W electrode in LiCl-KCl-BiCl₃ ($3.37 \times 10^{-6} \text{ mol cm}^{-3}$) melts before (black line) and after (red line) the addition of LaCl₃ ($8.67 \times 10^{-5} \text{ mol cm}^{-3}$); (b) Cyclic voltammograms obtained in LiCl-KCl-LaCl₃ ($8.67 \times 10^{-5} \text{ mol cm}^{-3}$)-BiCl₃ ($3.37 \times 10^{-6} \text{ mol cm}^{-3}$) melts at different terminal potentials at 773 K. Starting potential: 0.4 V; Scan rate: 0.1 V s^{-1} ; $S_{\text{W}} = 0.314 \text{ cm}^2$.

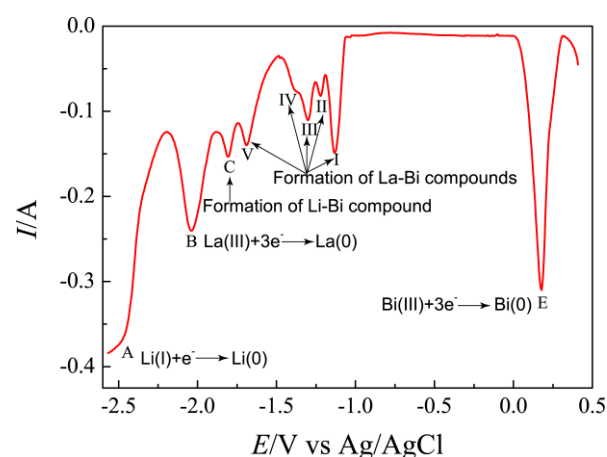


Fig. 7 Square wave voltammogram obtained in LiCl-KCl-LaCl₃ ($8.67 \times 10^{-5} \text{ mol cm}^{-3}$)-BiCl₃ ($3.37 \times 10^{-6} \text{ mol cm}^{-3}$) melts on a W electrode at 773 K. Potential step: 1 mV; frequency: 20Hz; $S_{\text{W}} = 0.314 \text{ cm}^2$.

square wave voltammetry was employed to study the electrochemical behavior of La(III) on a Bi coated W electrode. Fig. 7 shows square wave voltammograms of La(III) in LiCl-KCl melts on a Bi coated W electrode at a step potential of 1 mV and frequency of 20 Hz at 773 K. Nine obvious peaks are observed. According to the reduction potentials of La and Li on a Bi coated W electrode in Fig. 6, the attribution of nine peaks could be confirmed. In addition to peaks A, B, and E, corresponding to the reactions of Li(I)/Li, La(III)/La and Bi(III)/Bi, respectively, the cathodic signal C, at about -1.80 V, is ascribed to the formation of Li-Bi alloy compound. The five peaks I, II, III, IV and V, identified at -1.14 V, -1.21 V, -1.30 V, -1.38 V and -1.69 V, correspond to the formation of five different La-Bi intermetallic compounds, respectively. Using square wave voltammetry, we can confirm the peak potentials of cathodic peaks I, II and III in Fig. 6(b).

Open circuit chronopotentiometry. -Thermodynamic properties of La-Bi intermetallic compounds

Adopting open circuit chronopotentiometry, as an appropriate electrochemical technique for the study of underlying alloys formation and dissolution, a thin layer specimen was prepared by cathodic deposition on a W electrode for short periods in the melts. The open-circuit potential of the electrode was registered vs time (as shown in Fig. 8). During this process, potential plateaus are associated with the state where two phases coexist at the electrode surface. Curve a (red curve) in Fig. 8 shows an open circuit chronopotentiogram obtained in the LiCl-KCl-BiCl₃ (3.37 × 10⁻⁶ mol cm⁻³) melts on a W electrode while applying a deposition potential of -2.50 V for 60 s. In the beginning, the potential stays at around -2.35 V (plateau A), which is interpreted due to the presence of deposited Li metal on the electrode and related to the Li(I)/Li(0) redox couple. After that, plateau C is correlated with the formation

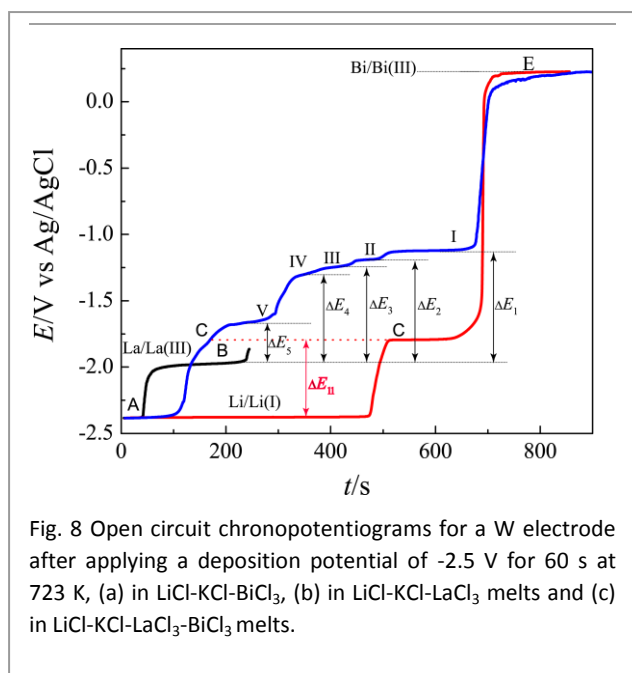
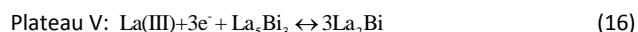
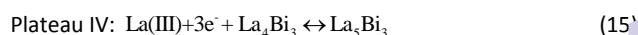
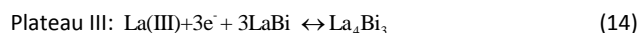
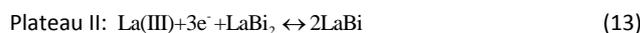
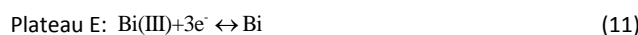
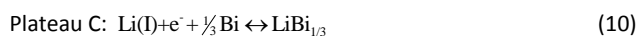
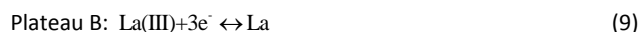


Fig. 8 Open circuit chronopotentiograms for a W electrode after applying a deposition potential of -2.5 V for 60 s at 723 K, (a) in LiCl-KCl-BiCl₃, (b) in LiCl-KCl-LaCl₃ melts and (c) in LiCl-KCl-LaCl₃-BiCl₃ melts.

of Li-Bi alloy. According to the below electrolysis results, the Li-Bi intermetallic compound is Li₃Bi characterized by XRD. The redox potential at 0.20 V is associated with the Bi(III)/Bi(0) system. Curve b (black curve) presents an open circuit chronopotentiogram obtained in the LiCl-KCl-LaCl₃ (8.67 × 10⁻⁵ mol cm⁻³) melts on a W electrode with applying a deposition potential of -2.50 V for 60 s. Except for the plateau A, a new plateau B observed, is ascribed to the La(III)/La(0) redox couple. Curve c (blue curve) illustrates the open circuit chronopotentiogram carried out in the LiCl-KCl-LaCl₃-BiCl₃ (8.67 × 10⁻⁵ mol cm⁻³)-BiCl₃ (3.37 × 10⁻⁶ mol cm⁻³) melts after affording a deposition potential of -2.5 V for 60 s. In curve c, five new plateaus, I, II, III, IV and V, are observed, corresponding to the two phases coexisting of five different La-Bi intermetallic compounds, respectively.

The equilibrium potentials measured with reference to the Ag/AgCl couple were converted to the electromotive forces (emf) against M(0) (M=La, Li), making it possible to estimate the standard molar Gibbs energies of formation for M-Bi (M=La, Li) intermetallics.^{12,13,21,38}

Therefore the plateaus (in Fig. 8) could be considered to correspond to the following reactions:



The emf corresponding to the chemical composition of M-Bi (M=La, Li) alloys is related to the activity of M (M=La, Li), by the expression:

$$emf = \Delta E = -\frac{RT}{3F} \ln a_M \quad (17)$$

where a_M is the activity of M (M=La, Li) in the M-Bi intermetallic compounds, taking pure M (M=La, Li) as the standard state.

The relative partial molar Gibbs free energies of La in the La-Bi intermetallic compounds, were also calculated from the obtained emf, ΔE vs (La(III)/La)/V, by the following equations:

$$\Delta \bar{G}_{\text{La}} = -3F \Delta E = RT \ln a_{\text{La}} \quad (18)$$

$\Delta \bar{G}_{\text{La}}$ is the relative partial molar Gibbs energy of La in the La-Bi intermetallic compound.

The values obtained at different temperatures are given in Table 2 and Table 3. The a_{Li} in the two-phase coexisting states between Li₃Bi and Li was found to be in the order of 10⁻⁵ to 10⁻⁴ as shown in Table 2. They are larger than the activities of La in La-Bi alloys in Table 3.

And the standard Gibbs energy of formation of Li₃Bi, $\Delta G_f^0(\text{Li}_3\text{Bi})$ can be calculated from the emf by the relation:

Table 2 Thermodynamic properties of Li in the two-phase coexisting states between Li₃Bi and Bi at different temperatures.

T(K)	E(V) vs Li(l)/Li	$\Delta G_f^0(\text{Li}_3\text{Bi})/\text{kJ mol}^{-1}$	a_{Li}	$\Delta G_f^0(T)/\text{kJ mol}^{-1}$
723	0.584±0.003	-169.07±0.87	8.48×10^{-5}	-225.33±0.077T
748	0.578±0.005	-167.33±1.45	1.27×10^{-4}	
773	0.572±0.004	-165.59±1.16	1.86×10^{-4}	
798	0.565±0.003	-163.57±0.87	2.70×10^{-4}	-255.40±0.059T ³⁹
823	0.557±0.004	-161.25±1.16	3.88×10^{-4}	

$$\Delta G_f^0(\text{Li}_3\text{Bi}) = -3F\Delta E_{\text{II}} \quad (19)$$

The temperature dependence of the emf is measured, and the variation of the Gibbs energy of formation of Li₃Bi with the temperature ($\Delta G_f^0(T)$) is also presented in Table 2. Weppner and Huggins³⁹ determined the Gibbs energy of formation of Li-Bi intermetallic compounds in the temperature range between 628 K and 873 K by emf method. Compared with their data, our experimental data are different, with a relative deviation of 11%.

The possible reasons are attributed to the different experimental condition.

The standard molar Gibbs energies of formation ΔG_f^0 for La-Bi intermetallic compound are calculated by the equation listed in Table 4. Morisson and Petot⁴⁰ determined the thermodynamic properties of LaBi₂ in CaF₂-LaF₃ melts in the temperature range of 823-1023 K using emf measurements. The value of Gibbs energy of formation for LaBi₂ at 823 K is very close to our experiment result. The linear dependence of the energy of formation, of the different

Table 3 Thermodynamic properties of La for La-Bi intermetallic compounds in two-phase coexisting states at various temperatures.

T/K	E_{eq}/V vs Ag/AgCl	$\Delta E/V$ vs La(III)/La	$\Delta G_{\text{La}}/\text{kJ (mol La)}^{-1}$	a_{La}
Plateau (La)				
723	-1.968±0.003			
748	-1.961±0.003			
773	-1.950±0.002			
798	-1.939±0.002			
823	-1.921±0.001			
Plateau I				
723	-1.122±0.003	0.846±0.006	-244.92±1.74	2.03×10^{-18}
748	-1.118±0.002	0.843±0.005	-244.05±1.45	9.08×10^{-18}
773	-1.109±0.002	0.841±0.004	-243.47±1.16	3.54×10^{-17}
798	-1.102±0.003	0.837±0.005	-242.31±1.45	1.38×10^{-16}
823	-1.099±0.001	0.822±0.002	-237.97±0.58	7.86×10^{-16}
Plateau II				
723	-1.188±0.005	0.78±0.008	-225.81±2.32	4.83×10^{-17}
748	-1.182±0.004	0.779±0.007	-225.52±2.03	1.79×10^{-16}
773	-1.176±0.006	0.774±0.008	-223.49±2.32	7.86×10^{-16}
798	-1.171±0.003	0.768±0.005	-221.47±1.45	3.17×10^{-15}
823	-1.164±0.004	0.757±0.005	-219.15±1.45	1.23×10^{-14}
Plateau III				
723	-1.240±0.001	0.728±0.004	-210.76±1.16	5.94×10^{-16}
748	-1.234±0.003	0.727±0.006	-210.47±1.74	2.01×10^{-15}
773	-1.231±0.002	0.719±0.004	-208.15±1.16	8.57×10^{-15}
798	-1.226±0.004	0.713±0.006	-206.41±1.74	3.08×10^{-14}
823	-1.216±0.006	0.705±0.007	-204.10±2.03	1.11×10^{-13}
Plateau IV				
723	-1.284±0.006	0.684±0.009	-198.02±2.61	4.95×10^{-15}
748	-1.278±0.004	0.683±0.007	-197.73±2.03	1.56×10^{-14}
773	-1.269±0.005	0.681±0.007	-197.15±2.03	5.24×10^{-14}
798	-1.261±0.006	0.678±0.008	-196.28±2.32	1.10×10^{-13}
823	-1.247±0.007	0.674±0.008	-195.12±2.32	4.11×10^{-13}
Plateau V				
723	-1.656±0.001	0.312±0.004	-90.32±1.16	2.97×10^{-7}
748	-1.650±0.003	0.311±0.006	-90.04±1.74	5.15×10^{-7}
773	-1.644±0.002	0.306±0.004	-88.59±1.16	1.04×10^{-6}
798	-1.642±0.002	0.297±0.004	-85.98±1.16	2.35×10^{-6}
823	-1.639±0.002	0.282±0.003	-81.68±0.87	6.33×10^{-6}

Table 4 Standard molar Gibbs energies of formation for La-Bi intermetallic compounds

Intermetallic compound	Equation	T /K	$\Delta G_f^\ominus/\text{kJ mol}^{-1}$	$\Delta G_f^\ominus(T)/\text{kJ mol}^{-1}$
LaBi ₂	$\Delta G_f^\ominus(\text{LaBi}_2) = -3F\Delta E_1$	723	-244.92±1.74	-269.22±0.033T
		748	-244.05±1.45	
		773	-243.47±1.16	
		798	-242.31±1.45	
		823	-237.97±0.58	
			-236.29 ⁴⁰	
LaBi	$\Delta G_f^\ominus(\text{LaBi}) = \frac{1}{2}[\Delta G_f^\ominus(\text{LaBi}_2) - 3F\Delta E_2]$	723	-235.36±2.03	-269.55±0.047T
		748	-234.79±1.74	
		773	-233.48±1.74	
		798	-231.89±1.45	
		823	-228.56±1.01	
La ₄ Bi ₃	$\Delta G_f^\ominus(\text{La}_4\text{Bi}_3) = [3\Delta G_f^\ominus(\text{LaBi}) - 3F\Delta E_3]$	723	-916.85±7.24	-1065.20±0.20T
		748	-915.11±6.95	
		773	-908.60±6.37	
		798	-902.08±6.08	
		823	-889.78±5.07	
La ₅ Bi ₃	$\Delta G_f^\ominus(\text{La}_5\text{Bi}_3) = \Delta G_f^\ominus(\text{La}_4\text{Bi}_3) - 3F\Delta E_4$	723	-1114.87±9.84	-1280.12±0.23T
		748	-1112.84±8.97	
		773	-1105.75±8.40	
		798	-1098.37±8.40	
		823	-1084.90±7.38	
La ₂ Bi	$\Delta G_f^\ominus(\text{La}_2\text{Bi}) = \frac{1}{3}[\Delta G_f^\ominus(\text{La}_3\text{Bi}_3) - 3F\Delta E_5]$	723	-401.73±3.67	-470.96±0.094T
		748	-400.96±3.57	
		773	-398.11±3.18	
		798	-394.78±3.19	
		823	-388.86±2.75	

intermetallic compounds, with the temperatures, was also presented in Table 4.

Galvanostatic and potentiostatic electrolysis and characterization of the deposits

To confirm the underpotential deposition of La on liquid Bi, galvanostatic and potentiostatic electrolysis were carried out on a Bi coated W electrode in the LiCl-KCl-LaCl₃-BiCl₃ melts. The La-Bi alloys prepared were always residue-shaped in molten salts whether at low or high temperature, we could not collect the La-Bi alloys. Therefore, galvanostatic and potentiostatic electrolysis were executed on a liquid Bi pool electrode in the LiCl-KCl-LaCl₃ melts. Fig. 9 shows SEM image and XRD pattern of alloy sample obtained by galvanostatic electrolysis (-0.1 A) for 8 h in LiCl-KCl-LaCl₃ (3.7×10^{-4} mol cm⁻³) melts on a liquid Bi pool electrode. The XRD pattern shows that the sample is comprised of LaBi₂, LaBi, Li₃Bi and Bi phases. Fig. 10 shows XRD pattern of alloy samples obtained by potentiostatic electrolysis at -1.4 V in LiCl-KCl-LaCl₃ (3.7×10^{-4} mol cm⁻³) melts on a liquid Bi pool electrode for 4 h and 6 h, respectively. The XRD patterns show the formation of different La-Bi intermetallic compounds. La-rich compound, La₂Bi, can be obtained by potentiostatic electrolysis with increasing the electrolysis time, but intermetallic compounds, La₄Bi₃ and La₅Bi₃, do not produced under our experimental conditions.

Conclusion

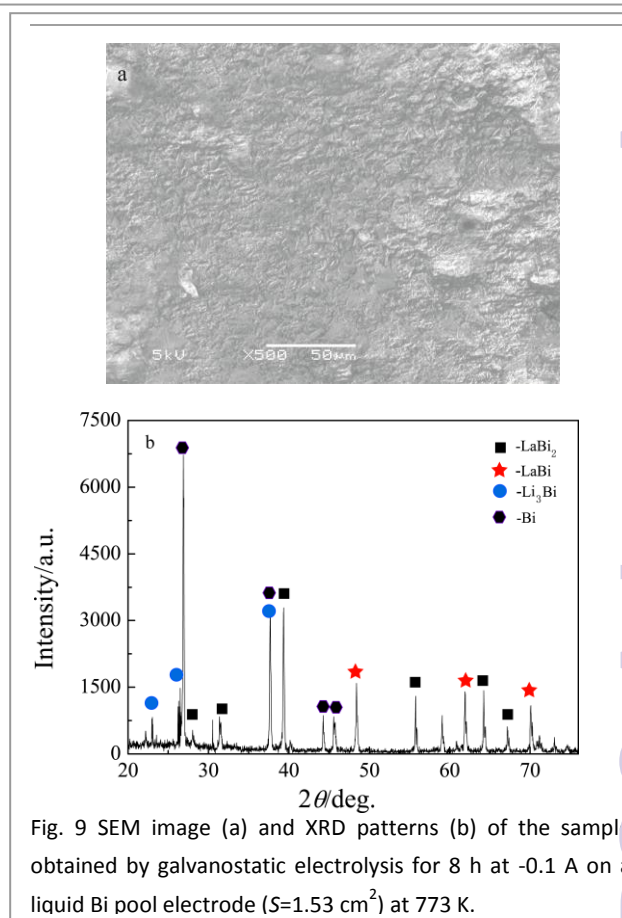


Fig. 9 SEM image (a) and XRD patterns (b) of the sample obtained by galvanostatic electrolysis for 8 h at -0.1 A on a liquid Bi pool electrode ($S=1.53 \text{ cm}^2$) at 773 K.

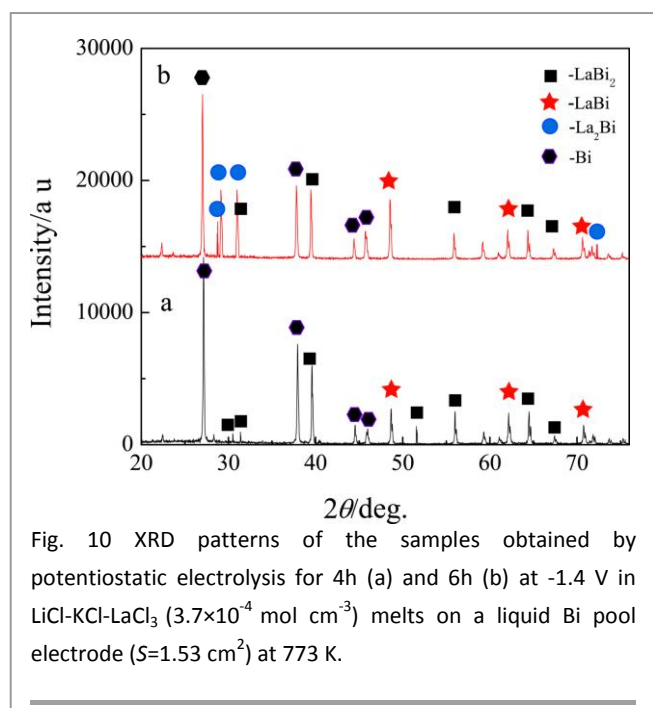


Fig. 10 XRD patterns of the samples obtained by potentiostatic electrolysis for 4h (a) and 6h (b) at -1.4 V in LiCl-KCl-LaCl₃ (3.7×10^{-4} mol cm⁻³) melts on a liquid Bi pool electrode ($S=1.53$ cm²) at 773 K.

The electrochemical behavior of La (III) was investigated in LiCl-KCl-LaCl₃ melts using a series of electrochemical techniques on liquid Bi electrodes (i.e. Bi pool and Bi coated W electrodes) at 773 K. The redox potentials of the La(III)/La couple on a liquid Bi electrode were observed at more positive potential values than that on an inert W electrode. This potential shift was due to a lowering of activity of La in liquid Bi phase caused by the formation of La-Bi intermetallic compounds. The diffusion coefficient of La in liquid Bi phase was measured by chronopotentiometry and was found to be 1.81×10^{-5} cm² s⁻¹.

Electromotive force, emf, measurements for different intermetallic compounds in two-phase coexisting states were carried out in the temperature range of 723-823 K. The activities of M (M=La, Li) in the M-Bi intermetallic compounds as well as the Gibbs energy of formation for M-Bi (M=La, Li) intermetallic compounds, LaBi₂, LaBi, La₄Bi₃, La₅Bi₃, La₂Bi, and Li₃Bi were obtained. The linear dependence of the standard molar Gibbs energies of formation of M-Bi (M=La, Li) intermetallic compounds with temperature was presented.

La-Bi and La-Li-Bi alloys were directly fabricated by potentiostatic and galvanostatic electrolysis on a liquid Bi pool electrode in LiCl-KCl-LaCl₃ melts at 773 K. LaBi₂, LaBi and La₂Bi phases, characterized by XRD, in bulk La-Bi alloys which were obtained by potentiostatic electrolysis. During the process of galvanostatic electrolysis, La-Li-Bi alloys obtained were comprised of LaBi₂, LaBi and Li₃Bi phases.

Acknowledgements:

The work was financially supported by Key Laboratory of Superlight Materials and Surface Technology, Ministry of Education, the National Natural Science foundation of China (21271054, 11575047 and 21173060), the Major Research plan of the National Natural Science Foundation of China (91326113 and 91226201), the Fundamental Research funds for the Central Universities (HEUCF201503007) and the International Exchange Program of

Harbin Engineering University for Innovation-oriented Talents Cultivation.

References

- 1 M. Gibilaro, L. Massot, R. Chamelot and P. Taxil, *Electrochim. Acta*, 2009, **54**, 5300-5306.
- 2 K. Kinoshita, K. Tadafumi, I. Tadashi, M. Ougier and J. P. Glatz, *J. Phys. Chem. Solids*, 2005, **66**, 619-624.
- 3 P. Soucek, L. Cassayre, R. Malmbeck, E. Mendes, R. Jardin and J. P. Glatz, *Radiochim. Acta*, 2008, **96**, 315-322.
- 4 O. Shirai, T. Iwai, K. Shiozawa, Y. Suzuki, Y. Sakamura and T. Inoue, *J. Nucl. Mater.*, 2000, **277**, 226-230.
- 5 H.F. McFarlane and M.J. Lineberry, *Prog. Nucl. Energ.*, 1997, **31**, 111-129.
- 6 M. Iizuka, K. Uozumi, T. Inoue, T. Iwai, O. Shirai and Y. Arai, *J. Nucl. Mater.*, 2001, **299**, 32-42.
- 7 K. Uozumi, M. Iizuka, T. Kato, T. Inoue, O. Shirai, T. Iwai and Y. Arai, *J. Nucl. Mater.*, 2004, **325**, 34-43.
- 8 O. Conocar, N. Douyere, J. P. Glatz, J. Lacquement, R. Malmbeck and J. Serp, *Nucl. Sci. Eng.*, 2006, **153**, 253-261.
- 9 K. Kinoshita, T. Inoue, S.P. Fusselman, D.L. Grimmer, J.J. Roy, R.L. Gay, C.L. Krueger, C.R. Nabelek and T.S. Storvick, *J. Nucl. Sci. Technol.*, 1999, **36**, 189-197.
- 10 M. Gibilaro, S. Bolmont, L. Massot, L. Latapie and P. Chamelot, *J. Electroanal. Chem.*, 2014, **726**, 84-90.
- 11 T. Murakami and T. Koyama, *J. Electrochem. Soc.*, 2011, **158**, F147-F153.
- 12 S. H. Kim, S. Paek, T. J. Kim, D. Y. Park and D. H. Ahn, *Electrochim. Acta*, 2012, **85**, 332-335.
- 13 Y. Castrillejo, M. R. Bermejo, P. Díaz Arocas, A. M. Martínez and E. Barrado, *J. Electroanal. Chem.*, 2005, **579**, 343-358.
- 14 S. Vandarkuzhali, M. Chandra, S. Ghosh, N. Samanta, S. Nedumaran, B. P. Reddy and K. Nagarajan, *Electrochim. Acta*, 2014, **145**, 86-98.
- 15 Y. Castrillejo, P. Hernández, R. Fernández and E. Barrado, *Electrochim. Acta*, 2014, **147**, 743-751.
- 16 G. Y. Kim, D. Yoon, S. Paek, S. H. Kim, T. J. Kim and D. H. Ahn, *J. Electroanal. Chem.*, 2012, **682**, 128-135.
- 17 K. Uozumi, M. Iizuka, T. Kato, T. Inoue, O. Shirai, T. Iwai and Y. Arai, *J. Nucl. Mater.*, 2004, **325**, 34-43.
- 18 O. Shirai, M. Iizuka, T. Iwai, Y. Suzuki and Y. Arai, *J. Electroanal. Chem.*, 2000, **490**, 31-36.
- 19 O. Shirai, K. Uozumi, T. Iwai and Y. Arai, *J. Appl. Electrochem.*, 2004, **34**, 323-330.
- 20 T. Kato, T. Inoue, T. Iwai and Y. Arai, *J. Nucl. Mater.*, 2006, **357**, 105-114.
- 21 Y. Castrillejo, M. R. Bermejo, P. Diaz Arocas, F. De La Rosa and E. Barrado, *Electrochemistry*, 2005, **73**, 636-643.
- 22 O. Shirai, M. Iizuka, T. Iwai and Y. Arai, *Anal. Sci.*, 2001, **17**, 51-57.
- 23 P. Chamelot, L. Massot, L. Cassayre and P. Taxil, *Electrochim. Acta*, 2010, **55**, 4758-4764.
- 24 K. Liu, L.Y. Yuan, Y. L. Liu, X. L. Zhao, H. He, G. A. Ye, Z. F. Chai and W. Q. Shi, *Electrochim. Acta*, 2014, **130**, 650-659.
- 25 F. Lantelme, T. Cartaller, Y. Berghoute, M. Hamdani, *Electrochem. Soc.*, 2001, **148**, C604-C613.
- 26 Y. Castrillejo, M. R. Bermejo, A. M. Martínez and P. Diaz Arcas, *J. Min. Metall. Sect. B-Metall.*, 2003, **39**, 109-135.
- 27 P. Masset, R.J.M. Konings, R. Malmbeck, J. Serp and J. P. Glatz, *J. Nucl. Mater.*, 2005, **344**, 173-179.
- 28 S. Vandarkuzhali, N. Gogoi, S. Ghosh, B. P. Reddy and K. Nagarajan, *Electrochim. Acta*, 2012, **59**, 245-255.
- 29 Y. L. Liu, L. Y. Yuan, G. A. Ye, K. Liu, L. Zhu, M. L. Zhang, Z. F. Chai and W. Q. Shi, *Electrochim. Acta*, 2014, **147**, 104-113.
- 30 H. Tang, B. Pesic, *Electrochim. Acta*, 2014, **119**, 120-130.
- 31 O. Shirai, A. Uehara, T. Fujii, H. Yamana, *J. Nucl. Mater.*, 2005, **344**, 142-145.

ARTICLE

Journal Name

- 32 J. Serp, P. Lefebvre, R. Malmbeck, J. Rebizant, P. Vallet, J. P. Glatz, *J. Nucl. Mater.*, 2005, **340**, 266-270.
- 33 G. Cordoba and C. Caravaca, *J. Electroanal. Chem.*, 2004, **572**, 145-151.
- 34 A. J. Bard and L. R. Faulkner, *Electrochemical Methods: Fundamentals and Applications*, John Wiley & Sons, New York, 2nd ed., 2001, 162.
- 35 W. Sutherland, *Phil. Mag.* 1905, **9**, 781-785.
- 36 *Handbook on Lead-Bismuth Eutectic Alloy and Lead Properties, Materials Compatibility*, Thermophysical and Electric Properties (Chapter 2), OECD Nuclear Energy Agency, 2007, 76.
- 37 K. A. Gschneidner and F. W. Calderwood, *Bull. Alloy Phase Diagrams*, 1989, **10**, 440-443.
- 38 M. Li, Q. Q. Gu, W. Han, Y. D. Yan, M. L. Zhang, Y. Sun and W. Q. Shi, *Electrochim. Acta*, 2015, **167**, 139-146.
- 39 W. Weppner and R. A. Huggins, *J. Electrochem Soc.*, 1978, **125**, 7-14.
- 40 A. Morisson and C. Petot, *Thermochim. Acta*, 1987, **115**, 167-173.

RSC Advances Accepted Manuscript